Electronic Supplementary Material (ESI) for Nanoscale.

Supplementary Information

for

Self-ordering of small-diameter metal nanoparticles by dewetting on hexagonal mesh templates

Eric R. Meshot[1,2], Zhouzhou Zhao[1],Wei Lu[1], and A. John Hart[1,3]*

[1] Department of Mechanical Engineering, University of Michigan, 2350 Hayward St., Ann Arbor, MI 48109, USA.

[2] Physical and Life Sciences Directorate, Lawrence Livermore National Laboratory, 7000 East Avenue, Livermore, CA 94551, USA.

[3] Mechanosynthesis Group, Department of Mechanical Engineering, Massachusetts Institute of Technology, Cambridge, MA 02139, USA.

*E-mail: ajhart@mit.edu

Experimental

The Fe thin film was deposited by sputtering, and the thickness was verified ex situ with AFM. For studies on hexagonal templates, films were deposited on commercially purchased AAO substrates (Synkera), which were received heat-treated so as to prevent a phase transition during annealing studies. Alternatively, for control experiments, 10 nm of alumina was sputtered on (100) Si wafers that were coated with 300 nm of thermal oxide. We performed annealing experiments in a single-zone, hot-wall tube furnace (Thermo-Fisher Minimite) at atmospheric pressure. First, the sample was loaded, and the gas lines and tube volume were purged with ultra-high purity He to eliminate O_2 and H_2O in the system. Then, the furnace temperature was ramped to 775 °C at a rate of 75 °C min^{-1} and held for 10 min in steady H_2 and He flows (100 and 400 sccm, respectively). Finally, we rapidly cooled the sample by removing the quartz tube from the furnace while maintaining the same gas environment. For carbon nanotube (CNT) growth experiments, we followed the annealing step with a 10 min of $C_2H_4/H_2/He$ flows at 100/100/400 sccm, respectively. We found it was crucial to bake the sample under dry He flow for 1 hour between 100-200 °C in order to remove moisture absorbed in the nanoporous AAO before CNT growth. Characterization was performed using SEM (Philips XL30 FEG), AFM (Veeco Dimension Icon) and grazing-incidence small-angle X-ray scattering, or GISAXS (G1 station; Cornell High Energy Synchrotron Source).

GISAXS nondestructive method interrogates statistically significant populations of nanostructures (10^9) on surfaces.[1] An X-ray energy of 10 ± 0.1 keV was selected with synthetic multilayer optics (W/B4C, 27.1 Å d-spacing) with a beam height of about 100 μm, and we used a 2-D detector. The substrate was tilted toward the X-ray beam at an angle of incidence α_i of approximately 0.15 degrees (F, which is below the critical angle for total external reflection.

The particle order (from both our experimental AFM and simulation images) was determined using a custom code,[2] which reads images to automatically locate particles and tabulate size (height) and spacing. Using the spatial coordinates of the particles, we calculated an order parameter ranging between 0 (disordered) and 1 (perfect hexagonal ordering).[3]

Order parameter

The order parameter we adopted is often used in highly ordered atomic surface structures. [3] The expression is,

$$Q=\frac{1}{3N}\sum_{i=1}^{N}[\cos\frac{4\pi x_i}{\sqrt{3}\lambda_0}+\cos\frac{4\pi}{\sqrt{3}\lambda_0}(-\frac{x_i}{2}+\frac{\sqrt{3}y_i}{2})+\cos\frac{4\pi}{\sqrt{3}\lambda_0}(-\frac{x_i}{2}-\frac{\sqrt{3}y_i}{2})]$$

where N is the total number of the particle, λ_0 is the lattice parameter and (x_i, y_i) are the coordinates of each particle. There are two implicit variables and one explicit variable λ_0 in the Eq. (3.4), which will influence the value of order parameter. Since the actual values of the function depend on the choice of the coordinate system, the two implicit variables are the origin (x_0, y_0) and the orientation θ of the coordinate system. Here we are looking for a best fit between the image and an unknown perfect lattice, thereby we are actually looking for a "maximized" order parameter Q_{max} in a space that consists of λ_0, θ and (x_0, y_0). Specifically, we scan θ from 0 to 60°, λ_0 from $0.5\lambda_a$ to $1.5\lambda_a$ and (x_0, y_0) among all particle locations to find a maximum Q. (λ_a is the average particle spacing extracted from the sample)

Model and simulations

We consider a representative dewetting system: a liquid thin film on a substrate surface. The free energy of the system, G, involves the surface energy of the film and the van der Waals (VDW) interaction between the liquid film surface and the substrate. The expression is given by

$$G=\iint[\frac{\gamma}{2}(\nabla h)^2+V(h)]dA \qquad \text{[A]}$$

where h denotes the height of the thin film. The area integration extends over the substrate surface. The first term accounts for the surface energy, which is related to the surface tension of the film, γ. This term prefers a flat surface and thus stabilizes the thin film. The second term stands for the VDW interaction, where $V(h)=B/h^8-A/12\pi h^2$. Here A is the Hamaker constant and B is a constant accounting for the strength of short-range repulsion. When A>0, the free energy decreases if the thin film thickness h is reduced. Combining Eq. (A) with lubrication approximation of the Navier-Stokes equation gives the governing equation for film thickness evolution, namely $\partial h / \partial t = \nabla \cdot (M(h) \nabla p) / \eta$. Here η is the viscosity, $M(h) = h^3 / 3$ is the mobility factor and $p = -\gamma \nabla^2 h + dV / dh$. Although the precise physical state of nanoscale metal catalysts is controversial, the framework sufficiently describes the flow of high-mobility metal atoms during dewetting at elevated temperatures (i.e., by surface diffusion). This mobility factor M equals $h^3/3$ for a liquid and is constant for solid diffusion. The difference in our simulation studies between assuming liquid versus solid state would be in the kinetics (i.e., slower for solids), but the equilibrium state of the final particle arrays is the same regardless of our assumption of the film's physical state. Normalizing the length by initial film thickness h_0 and time by $t_0 = \eta h_0 / \gamma$, we have the following normalized equation

$$\partial h / \partial t = \nabla \cdot (m(h) \nabla p) \quad \text{[B]}$$

where $p = (-\nabla^2 h - 8B_0 / h^9 + A_0 / 6\pi h^3)$, and $B_0 = B / \gamma h_0^8$, $A_0 = A / \gamma h_0^2$ and $m(h) = h^3 / 3h_0^3$

To conduct the numerical simulation, we consider Eq. (B) in Fourier space,

$$\partial \hat{h} / \partial t = i\mathbf{k} \cdot \{\hat{m}(i\mathbf{k}\hat{p})_r\}_k \quad \text{[C]}$$

where the hat and subscript 'k' denote Fourier transform, 'r' denotes inverse Fourier transform, and $\mathbf{k}$ is the wave number vector. $\hat{p} = k^2 + (-8B_0 / h^9 + A_0 / 6\pi h^3)_k$. The second term is a nonlinear function of *h*, so $\hat{p}$ is calculated by numerical Fourier transform. To enhance numerical stability, we applied a semi-implicit method in our simulation for time integration. Specifically, we added a linear term, $\nabla^4 C$, to both sides so that Eq. (C) became $\partial \hat{h} / \partial t + k^4 \hat{h} = i\mathbf{k} \cdot \{\hat{m}(i\mathbf{k}\hat{p})_r\}_k + k^4 \hat{h}$. The $k^4 \hat{h}$ tem on the left side is evaluated at time (*n*+1) and the term on the right side is evaluated at time *n*. Denote the time step by Δt and replace $\partial \hat{h} / \partial t$ by $(\hat{h}^{(n+1)} - \hat{h}^{(n)}) / \Delta t$. The algorithm for *n*+1 time is given by

$(1+k^4\Delta t)\hat{h}^{(n+1)} = (1+k^4\Delta t)\hat{h}^{(n)} + \Delta t\ i\mathbf{k}\cdot\{\hat{m}(i\mathbf{k}\hat{p})_r\}_k{}^{(n)}$. This semi-implicit approach significantly alleviated the time step constraint.

Figures

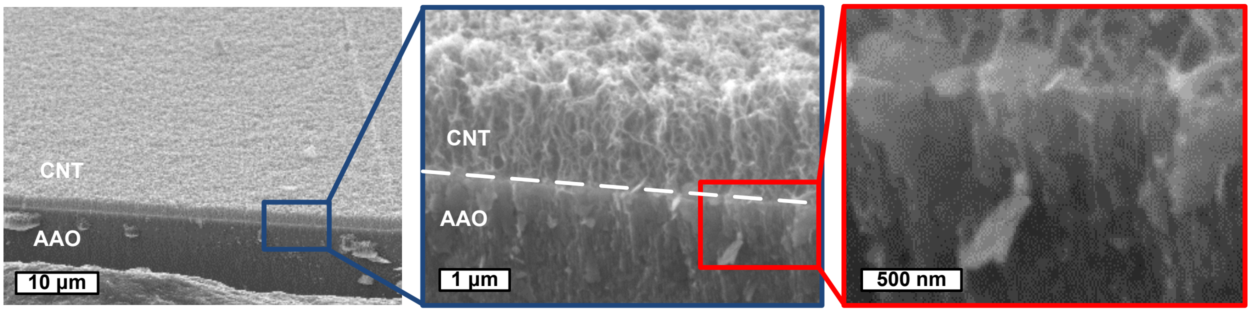

Figure S1. SEM imaging reveals that vertically aligned carbon nanotubes (CNTs) were uniformly synthesized from templated Fe catalyst nanoparticles (from 2 nm Fe film) across the AAO substrate (18-nm pore size, 49-nm spacing). The cross section shows that CNTs indeed originate from the top surface, with no evidence of CNTs within the porous structure of the AAO.

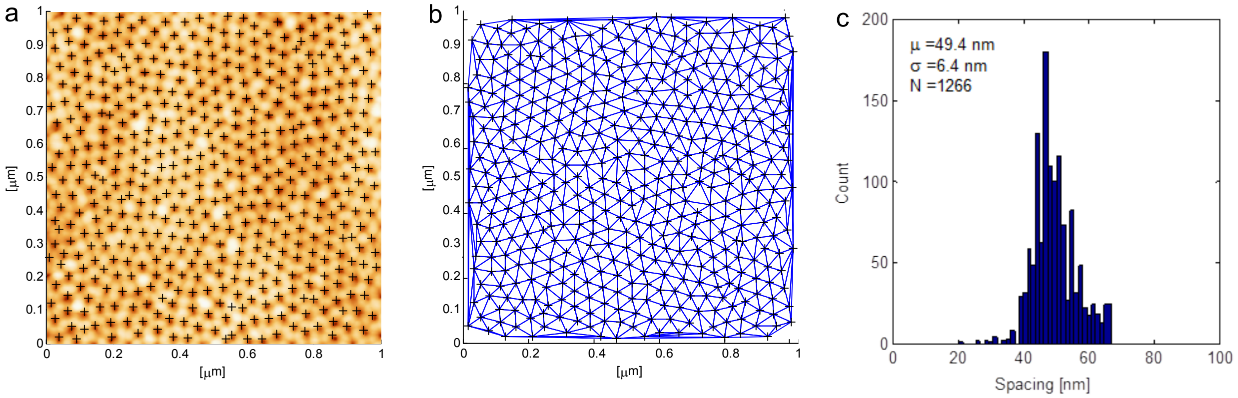

Figure. S2. Statistics for the center-to-center spacing between pores of a bare AAO substrate, as measure by AFM (image shown in Figure 2e). a) Pore locations indicated by + symbol, identified by finding local minima. b) Delaunay triangulation of the set of pore locations illustrates the center-to-center pore spacing, which is tabulated in panel c), where the number of bins = $\sqrt{N}$. The mean spacing of the AAO templates used in our study was 49 nm.

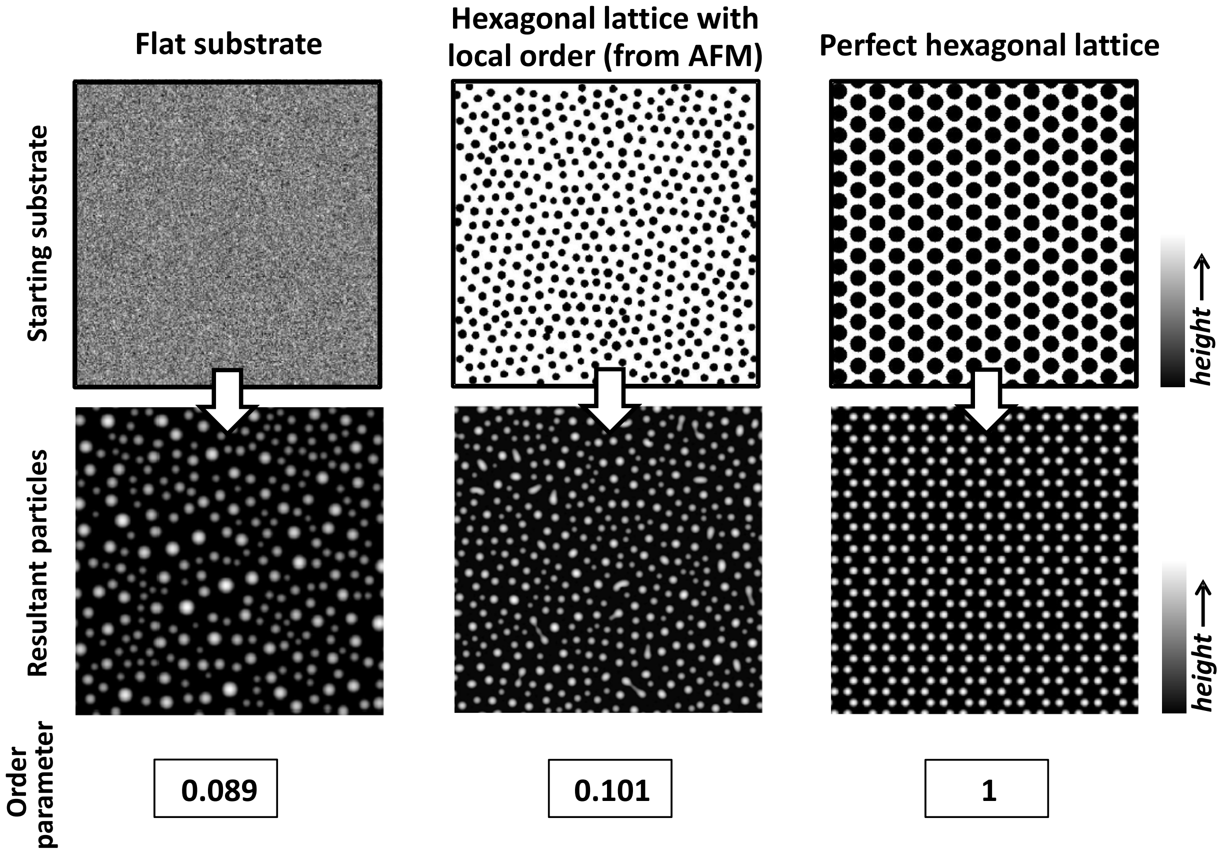

Figure S3. Comparison of dewetting on various simulated starting substrate topographies (shown in top row), including from left to right, flat (with random roughness), mesh (with pore location extracted directly from AFM data in Figure S2), and perfect mesh (with perfect hexagonal order). The bottom row shows the particle arrays that result from each case and the corresponding order parameter. Introducing the AAO pore structure yields a 10% enhancement in order above the flat case, while the perfect hexagonal pores unsurprisingly yield perfectly ordered particles. Simulations were performed with a mean pore size of 25 nm spaced by 50 nm.

References

1. Levine, J. R.; Cohen, J. B.; Chung, Y. W.; Georgopoulos, P., Grazing-incidence small-angle X-ray scattering: new tool for studying thin film growth. *Journal of Applied Crystallography* **1989,** *22* (6), 528-532.
2. Meshot, E. R.; Verploegen, E.; Bedewy, M.; Tawfick, S.; Woll, A. R.; Green, K. S.; Hromalik, M.; Koerner, L. J.; Philipp, H. T.; Tate, M. W.; Gruner, S. M.; Hart, A. J., High-Speed in Situ X-ray Scattering of Carbon Nanotube Film Nucleation and Self-Organization. *ACS Nano* **2012**.
3. Gong, H.; Lu, W.; Wang, L.; Li, G.; Zhang, S., The effects of substrate size and temperature on the deposition of Cu clusters on a Si substrate. *Journal of Applied Physics* **2012,** *112* (2).